Physics Letters B 702 (2011) 402–407

Contents lists available at ScienceDirect

Physics Letters B

www.elsevier.com/locate/physletb

Chirally motivated K^- nuclear potentials

A. Cieplý [a], E. Friedman [b], A. Gal [b,*], D. Gazda [a], J. Mareš [a]

[a] Nuclear Physics Institute, 25068 Řež, Czech Republic
[b] Racah Institute of Physics, The Hebrew University, 91904 Jerusalem, Israel

ARTICLE INFO

Article history:
Received 3 May 2011
Received in revised form 20 June 2011
Accepted 18 July 2011
Available online 23 July 2011
Editor: J.-P. Blaizot

Keywords:
Kaon–baryon interactions
Mesic nuclei
Mesonic atoms

ABSTRACT

In-medium subthreshold $\bar{K}N$ scattering amplitudes calculated within a chirally motivated meson–baryon coupled-channel model are used self consistently to confront K^- atom data across the periodic table. Substantially deeper K^- nuclear potentials are obtained compared to the shallow potentials derived in some approaches from threshold $\bar{K}N$ amplitudes, with $\mathrm{Re}\,V_{K^-}^{\mathrm{chiral}} = -(85 \pm 5)$ MeV at nuclear matter density. When $\bar{K}NN$ contributions are incorporated phenomenologically, a very deep K^- nuclear potential results, $\mathrm{Re}\,V_{K^-}^{\mathrm{chiral+phen.}} = -(180 \pm 5)$ MeV, in agreement with density dependent potentials obtained in purely phenomenological fits to the data. Self consistent dynamical calculations of K^-–nuclear quasibound states generated by $V_{K^-}^{\mathrm{chiral}}$ are reported and discussed.

1. Introduction

The interaction of K^- mesons with hadronic systems, ranging from K^- atoms through K^-–nuclear clusters to dense strange hadronic matter realized perhaps in neutron stars, is of topical interest [1]. SU(3) chiral symmetry combined with coupled channel techniques provides a theoretical framework in which low energy meson–baryon observables can be systematically evaluated. In such an approach the $\Lambda(1405)$ resonance, dominating the $\bar{K}N$–$\pi\Sigma$ physics at energies near the $\bar{K}N$ threshold, is generated dynamically. It is natural then to expect a strongly attractive and absorptive near-threshold K^-–nuclear interaction which might support K^-–nuclear clusters [2] and K^- condensation in compact stars [3]. A typical scale for the nuclear-matter depth of chirally motivated K^-–nuclear potentials is 100 MeV [4], although considerably shallower potentials have also been derived [5]. Outside of chirally motivated interaction models, suggestions were put forward for much stronger potentials that could lead eventually to fairly narrow quasibound K^-–nuclear clusters once the strong transition $\bar{K}N \to \pi\Sigma$ is kinematically forbidden [6]. These suggestions have stimulated experimental searches, the best known of which claiming rather broad signals of a deeply bound K^-pp configuration, at and below the $\pi\Sigma N$ threshold [7,8]. If these claims are substantiated in dedicated experiments, it would appear unavoidable to conclude that the K^-–nuclear potential depth is considerably greater than 100 MeV.[1] It would also imply a rather strong two-nucleon non-mesonic absorption mode $\bar{K}NN \to YN$ ($Y \equiv \Lambda, \Sigma$), considerably beyond a chiral-model estimate $\Gamma \approx 22$ MeV for a single-nucleon induced $\Lambda(1405)N \to YN$ conversion [11]. In the present Letter we focus on the use of in-medium chirally motivated K^-–nuclear potentials in kaonic atoms and discuss the constraints provided by a self consistent analysis of kaonic atom data.

Strong interaction level shifts and widths in kaonic atoms present a unique source of information on the K^-–nuclear interaction at threshold [12]. Phenomenological analyses of large data sets encompassing the whole periodic table, using optical potentials, reveal characteristic features of the interaction. These could reflect on the underlying K^-N interaction in the medium, in particular its energy and density dependence. Phenomenological density-dependent K^-N scattering amplitudes allow for very good fits to kaonic atom data [13,14] but the depths of the real optical potential are typically up to four times larger than what some in-medium chiral models predict at threshold [5]. Another feature of empirical kaonic atom optical potentials is that the real part is *compressed* relative to the corresponding nuclear density, with r.m.s. radius smaller than the nuclear r.m.s. radius. The reverse is true for the imaginary part. It is shown below that these are natural consequences of the density dependence of the present chiral model in-medium amplitudes.

[1] The distinction between deep ($\gtrsim 150$ MeV) and shallow ($\lesssim 50$ MeV) K^-–nuclear potentials has been recently discussed within Λ hypernuclear formation rate calculations [9] which were found to slightly favor a deep potential interpretation of recent FINUDA spectra [10].

* Corresponding author.
E-mail address: avragal@vms.huji.ac.il (A. Gal).

0370-2693
doi:10.1016/j.physletb.2011.07.040

The Klein–Gordon (KG) dispersion relation satisfied by K^- mesons in medium of density ρ is of the form

$$\omega_K^2 - \vec{p}_K^{\,2} - m_K^2 - \Pi_K(\omega_K, \rho) = 0, \tag{1}$$

where $\Pi_K(\omega_K, \rho) = 2(\mathrm{Re}\,\omega_K)V_{K^-}$ is the self energy (SE) operator for a K^- meson with momentum $\vec{p}_K$ and energy ω_K. A $\vec{p}_K$ momentum dependence of Π_K is suppressed since, as is shown below, it may be transformed into density and energy dependence. In terms of the in-medium K^-N c.m. forward scattering amplitude $F_{K^-N}(\sqrt{s}, \rho)$ (here assumed s-wave):

$$\Pi_K(\omega_K, \rho) \approx -4\pi\left(1 + \frac{\omega_K}{m_N}\right)F_{K^-N}(\sqrt{s}, \rho)\rho, \tag{2}$$

where $s = (E_K + E_N)^2 - (\vec{p}_K + \vec{p}_N)^2$ is the Lorentz invariant Mandelstam variable s which reduces to the square of the total K^-N energy in the two-body c.m. frame and m_N is the nucleon mass. In the laboratory frame, $E_K = \omega_K$. The KG dispersion relation (1) in bound state applications for a K^- meson leads to a KG equation satisfied by the K^- wavefunction [12]:

$$\left[\nabla^2 - 2\mu(\mathcal{B}_K + V_c) + (V_c + \mathcal{B}_K)^2 + 4\pi\left(1 + \frac{m_K - B_K}{m_N}\right)F_{K^-N}(\sqrt{s}, \rho)\rho\right]\psi = 0, \tag{3}$$

where μ is the K^-–nucleus reduced mass, V_c is the Coulomb potential generated by the finite-size nuclear charge distribution, and $\mathcal{B}_K = B_K + \mathrm{i}\Gamma_K/2$ is a complex binding energy, including a strong interaction width Γ_K. Finite-medium corrections are applied in our calculations specifically to the coefficient of F_{K^-N} in Eq. (3).

Wycech [15] and Bardeen and Torigoe [16] suggested long time ago within $\Lambda(1405)$-based phenomenological models that *subthreshold* K^-N scattering amplitudes are relevant in kaonic atom studies, where the kaon energy is essentially at threshold. In the present Letter we construct the K^- meson SE operator (2) near threshold ($\omega_K \approx m_K$) from in-medium subthreshold K^-N scattering amplitudes derived within a chirally motivated meson–baryon coupled-channel separable-potential model [17]. It is shown for the first time how the energy and density dependence of $F_{K^-N}(\sqrt{s}, \rho)$ leads to a deep K^-–nuclear potential V_{K^-} in kaonic atoms. This conclusion holds already at the lowest-order Tomozawa–Weinberg level that provides excellent starting point for modern chiral models [2]. We also report on self-consistent calculations of K^- quasibound nuclear states based on in-medium extensions of the free-space model of Ref. [17]. The calculated binding energies and widths are compared with similar entities calculated in Ref. [18].

2. Subthreshold energy and density dependence

The present calculations are based on the chirally motivated meson–baryon coupled-channel separable-potential model of Ref. [17]. This free-space model expands consistently and systematically to next-to-leading-order (NLO) within the heavy baryon formulation of chiral perturbation theory. The low-energy constants of the model are fitted to low energy K^-p scattering and reaction data. The free-space K^-N scattering amplitude F_{K^-N} is given then in a separable form:

$$F_{K^-N} = g(k) f_{K^-N}(\sqrt{s})\, g(k'), \quad g(k) = \frac{\alpha^2}{k^2 + \alpha^2}, \tag{4}$$

with c.m. momenta $\vec{k}$, $\vec{k}'$. Of the several versions specified in Table 3 of Ref. [17], we chose the one with a range parameter

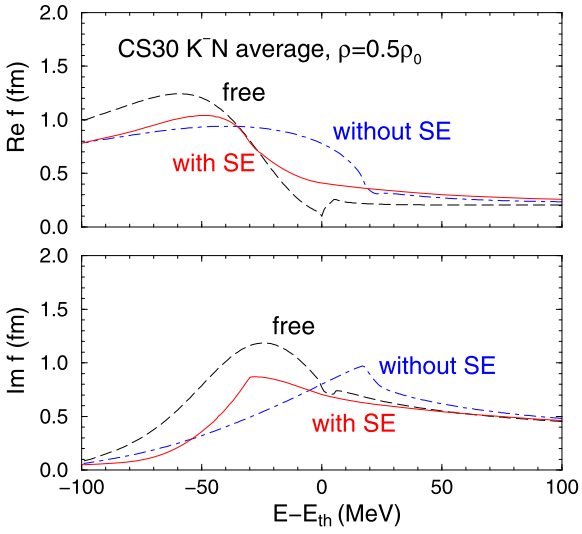

Fig. 1. Energy dependence of the c.m. K^-N reduced amplitude (5) in version CS30 of the chiral model [17] below and above $E_{\mathrm{th}} = m_K + m_N = 1432$ MeV. Dashed curves: free-space amplitude; dot-dashed curves: Pauli blocked amplitude at $0.5\rho_0$; solid curves: including meson and baryon self energies (SE), also at $0.5\rho_0$.

$\alpha = 639$ MeV.[2] Other chirally motivated potential models that start with zero range, i.e. no momentum dependence, in practical applications often introduce at least implicitly a finite range, e.g., a cutoff momentum $q_{\mathrm{max}} = 630$ MeV [5] or a renormalization scale $\mu = 630$ MeV [20]. The momentum dependence of the amplitude F_{K^-N} in the separable-potential model of Ref. [17] is rather weak for the applications discussed in the present work and is secondary to the strong energy dependence generated by the $\Lambda(1405)$ resonance.

A typical resonance-shape energy dependence is shown in Fig. 1 by dashed lines (marked 'free') for the *reduced* scattering amplitude

$$f_{K^-N}(\sqrt{s}) = \frac{1}{2}\left[f_{K^-p}(\sqrt{s}) + f_{K^-n}(\sqrt{s})\right] \tag{5}$$

which is appropriate for the interaction of K^- mesons with symmetric nuclear matter. The imaginary part peaks about 25 MeV below the $\bar{K}N$ threshold, and the real part rapidly varies there from weak attraction above to strong attraction below threshold. While $f_{K^-N}(\sqrt{s})$ at and near threshold is constrained by data that serve to determine the parameters of the chiral model, the extrapolation to the subthreshold region suffers from ambiguities and depends on the applied model [2]. The free-space reduced scattering amplitude shown in Fig. 1 is quantitatively similar to the corresponding K^-N scattering amplitudes in other chirally motivated models exhibited in Fig. 7 of Ref. [20].

Also shown in Fig. 1 is the energy dependence of two in-medium versions of $f_{K^-N}(\sqrt{s}, \rho = 0.5\rho_0)$. One version, in dot-dashed lines (marked 'without SE'), follows Ref. [4] to require Pauli blocking in the intermediate $\bar{K}N$ states for $\rho \neq 0$. The resulting f_{K^-N} exhibits now a resonance-like behavior about 20 MeV above threshold, in agreement with Ref. [4]. The other version, in solid lines (marked 'with SE'), follows Ref. [21] to add self consistently meson and baryon self energies in intermediate states, similarly to Refs. [5,22]. The resulting in-medium f_{K^-N} is strongly energy

[2] This version, labeled below CS30, produces two $I = 0$ S-matrix poles in the neighborhood of the $\bar{K}N$ threshold, the lower one at $\mathrm{Re}\,\sqrt{s} = 1398$ MeV evolves from the $\pi\Sigma$ channel, the upper one at 1441 MeV – from the $\bar{K}N$ channel, within the range of values provided by NLO chiral calculations, e.g., Ref. [19].

dependent below threshold, with a resonance-like behavior about 30 MeV below threshold. Similar results are obtained at full nuclear matter density $\rho_0 = 0.17$ fm^{-3}. We note that whereas the two in-medium reduced amplitudes shown in the figure are close to each other far below and far above threshold, they differ substantially at and near threshold. This applies also to the full amplitudes since the form factors $g(k)$ remain intact in the transition from free-space to in-medium separable amplitudes. At threshold, in particular, the real part of the 'with SE' amplitude is about half of that 'without SE', corresponding to a depth $-\mathrm{Re}\, V_{K^-}(\rho_0) \approx$ 40–50 MeV, in agreement with Ramos and Oset [5].

The c.m. reduced amplitudes are functions of $\sqrt{s}$. In the two-body c.m. system $\vec{p}_K + \vec{p}_N = 0$, but in the K^-–nucleus c.m. system (approximately nuclear laboratory system) $\vec{p}_K + \vec{p}_N \neq 0$. Averaging over angles yields $(\vec{p}_K + \vec{p}_N)^2 \to (p_K^2 + p_N^2)$. For bound hadrons we expand near threshold, neglecting quadratic terms in the binding energies $B_K = m_K - E_K$, $B_N = m_N - E_N$:

$$\sqrt{s} \approx E_{\mathrm{th}} - B_N - B_K - \xi_N \frac{p_N^2}{2m_N} - \xi_K \frac{p_K^2}{2m_K}, \tag{6}$$

where $\xi_{N(K)} = m_{N(K)}/(m_N + m_K)$. For the square of the relative momenta $\vec{k}$, $\vec{k}'$ in form factors g, Eq. (4), we again average on angles, yielding

$$k^2, k'^2 \to \xi_N \xi_K \left(2m_K \frac{p_N^2}{2m_N} + 2m_N \frac{p_K^2}{2m_K} \right). \tag{7}$$

Replacing in Eqs. (6) and (7) the kinetic energy $p_K^2/(2m_K)$ in the local density approximation by $-B_K - \mathrm{Re}\, \mathcal{V}_{K^-}(\rho)$ where $\mathcal{V}_{K^-} = V_{K^-} + V_c$, and approximating the nucleon kinetic energy $p_N^2/(2m_N)$ in the Fermi gas model by $23(\rho/\rho_0)^{2/3}$ MeV, Eq. (6) becomes

$$\sqrt{s} \approx E_{\mathrm{th}} - B_N - \xi_N B_K - 15.1 \left(\frac{\rho}{\rho_0} \right)^{2/3} + \xi_K\, \mathrm{Re}\, \mathcal{V}_{K^-}(\rho). \tag{8}$$

The downward energy shift invoked by Eq. (8), with respect to E_{th}, corresponds to that implied in the impulse approximation when the many-body $\bar{K}N$ amplitude evaluated at the threshold energy E_{th} is replaced by the two-body amplitude at the c.m. energy $\sqrt{s}$. Note its density dependence. In most of the subsequent discussion it is used as is, although we also checked the effect of implementing gauge invariance through the substitution $\sqrt{s} \to \sqrt{s} - V_c$. We note that gauge invariance was not implemented in the solution of the free-space Lippmann–Schwinger equations for the underlying chiral model of Ref. [17], nor in its in-medium extension displayed in Fig. 1.

For completeness, we comment on the range of momenta k, k' transcribed by Eq. (7). In naive applications to kaonic atoms where one assumes $p_K \approx 0$, these momenta are due to Fermi motion, as given by the first term on the r.h.s. of Eq. (7) which is bounded by $k(\rho_0), k'(\rho_0) \sim 72$ MeV, quite negligible compared to the momentum dependence scale $\alpha = 639$ MeV in model CS30. However, for strongly attractive K^- nuclear potentials, reaching depths of about 180 MeV in phenomenological studies [12], the second term on the r.h.s. of Eq. (7) dominates, yielding $k(\rho_0), k'(\rho_0) \sim 276$ MeV. These momenta are nonnegligible, but they are well within the CS30 momentum dependence scale $\alpha = 639$ MeV which emerged by fitting to $K^- p$ low-energy data.

3. Kaonic atoms

We now apply the method outlined above to the interaction of K^- mesons with nuclei close to threshold, as a means of testing the subthreshold chiral amplitude formalism against experimental

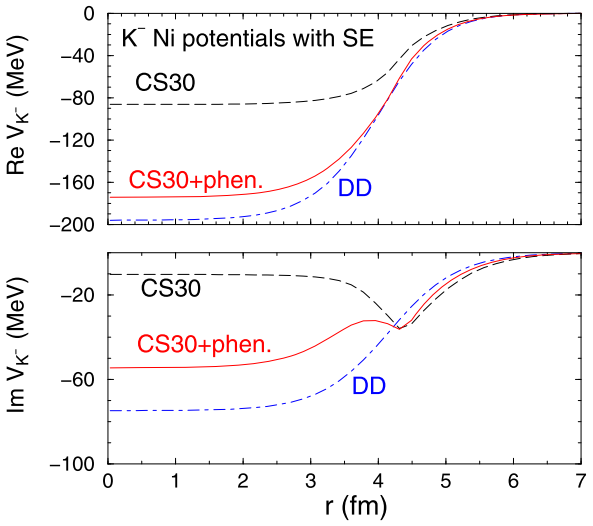

Fig. 2. K^-–nuclear potentials for K^- atoms of Ni. Dashed curves: derived self consistently from in-medium CS30 amplitudes; solid curves: plus phenomenological terms from global fits; dot-dashed curves: purely phenomenological DD potentials from global fits.

results. A distinction was made in solving the KG equation (3) between proton and neutron densities, replacing $F_{K^-N}(\sqrt{s}, \rho)\rho(r)$ by $\mathcal{F}^{\mathrm{eff}}_{K^-N}(\sqrt{s}, \rho)\rho(r)$, where

$$\mathcal{F}^{\mathrm{eff}}_{K^-N}(\sqrt{s}, \rho)\rho(r) = F_{K^-p}(\sqrt{s}, \rho)\rho_p(r) + F_{K^-n}(\sqrt{s}, \rho)\rho_n(r), \tag{9}$$

with ρ_p and ρ_n normalized to Z and N, respectively, and $Z + N = A$. The reduced amplitudes f_{K^-p} and f_{K^-n} were evaluated at $\sqrt{s}$ given by Eq. (8), where the atomic binding energy B_K was neglected with respect to $B_N \approx 8.5$ MeV. A similar approximation was made in Eq. (7) for k^2, k'^2. B_K was also neglected with respect to m_K in Eq. (3). The corresponding potential was calculated at each radial point for every target nucleus in the data base. Self consistency was required in solving Eq. (8) with respect to $\mathrm{Re}\, V_{K^-}$, i.e., the value of $\mathrm{Re}\, V_{K^-}(\rho)$ in the expression for $\sqrt{s}$ and in the form factors g had to agree with the resulting $\mathrm{Re}\, V_{K^-}(\rho)$.

Fig. 2 shows, as representative examples, several K^-–Ni potentials. The CS30 'with SE' amplitudes, within the self consistent procedure described above and without adjustable parameters, yield the potential marked CS30. For $\mathrm{Re}\, V_{K^-}$, similar depths to within a few MeV are obtained using CS30 'without SE' amplitudes. $\mathrm{Re}\, V^{\mathrm{CS30}}_{K^-}$ is twice deeper, −85 MeV with respect to −40 MeV, than the shallow potential (not shown here) used in the kaonic atom calculations of Ref. [23]. That shallow potential followed from a *threshold* value $f_{K^-N}(E_{\mathrm{th}}, \rho)$, without going subthreshold. Yet, $\mathrm{Re}\, V^{\mathrm{CS30}}_{K^-}$ is not as deep as $\mathrm{Re}\, V^{\mathrm{DD}}_{K^-}$, where the density dependent (DD) potential $V^{\mathrm{DD}}_{K^-}$, also shown in the figure, represents the best fit with $\chi^2 = 103$ for 65 data points obtained using purely phenomenological DD potentials [12].

The density dependence of the chiral CS30 'with SE' effective scattering amplitude $\mathcal{F}^{\mathrm{eff}}_{K^-N}$, calculated self consistently for Ni, is shown in Fig. 3. The increase of $\mathrm{Re}\, \mathcal{F}^{\mathrm{eff}}_{K^-N}(\rho)$ with density over the nuclear surface region combined with the decrease of $\mathrm{Im}\, \mathcal{F}^{\mathrm{eff}}_{K^-N}(\rho)$ is the underlying mechanism behind the compression and inflation of successful phenomenological best-fit potentials such as $V^{\mathrm{DD}}_{K^-}$ [13]. However, the decrease of $\mathrm{Im}\, \mathcal{F}^{\mathrm{eff}}_{K^-N}$ is unreasonably rapid, leading in the lower part of Fig. 2 to the peculiar shape of $\mathrm{Im}\, V^{\mathrm{CS30}}_{K^-}$

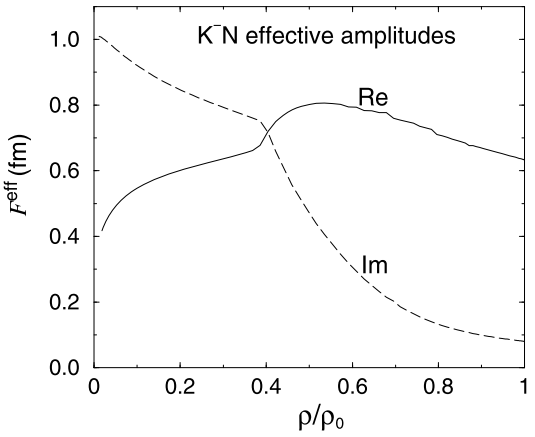

Fig. 3. Density dependence of the in-medium 'with SE' CS30 self consistent subthreshold amplitude $\mathcal{F}^{\rm eff}_{K^-N}$ for Ni.

at the nuclear surface.[3] A substantial K^-N energy shift into the subthreshold region is involved in the calculation of $\mathcal{F}^{\rm eff}_{K^-N}$, e.g., -40 MeV at $0.5\rho_0$ down to -60 MeV at ρ_0 in Ni. For such far subthreshold energies, the reduced amplitude $\mathrm{Im}\, f^{\rm CS30}_{K^-N}$, as seen in Fig. 1, is too small to provide the absorptivity required by the kaonic atom data. Note that these single-nucleon amplitudes do not account for multi-nucleon absorption which becomes increasingly important at subthreshold energies.

Fig. 2 also demonstrates the effect of adding adjustable ρ and ρ^2 terms to $V^{\rm CS30}_{K^-}$, resulting in a best-fit potential $V^{\rm CS30+phen.}_{K^-}$ with χ^2 of 164. For the imaginary part, the depth $-\mathrm{Im}\, V^{\rm CS30}_{K^-}(\rho_0)$ is substantially increased towards reaching $-\mathrm{Im}\, V^{\rm DD}_{K^-}(\rho_0)$, with a weaker bulge now at the nuclear surface. For the real part, the depth $-\mathrm{Re}\, V^{\rm CS30}_{K^-}(\rho_0)$ is also significantly increased from 85 MeV to 175 MeV, close to the phenomenological potential depth $-\mathrm{Re}\, V^{\rm DD}_{K^-}$. Similar results, to within a few MeV, hold when starting from the CS30 'without SE' amplitudes and also when the substitution $\sqrt{s} \to \sqrt{s} - V_c$ is made in the r.h.s. of Eq. (8). We note that the phenomenological addition to both $\mathrm{Im}\, V^{\rm CS30}_{K^-}$ and $\mathrm{Re}\, V^{\rm CS30}_{K^-}$ is dominated by ρ^2 terms which are required by the fit procedure and which are likely to represent $\bar{K}NN$ absorptive and dispersive contributions, respectively. The emerging phenomenology is similar to that for V_{π^-} in pionic atom studies where theoretically motivated single-nucleon contributions are augmented by phenomenological ρ^2 terms representing πNN processes [24]. More work is required to justify microscopically the size of the ρ^2 kaonic atom contributions suggested by the successful $V^{\rm CS30+phen.}_{K^-}$.

Although our study of kaonic atoms focused on K^-N s-wave interaction models incorporating the subthreshold $\Lambda(1405)$ resonance, we also checked whether p-wave contributions from the subthreshold $\Sigma(1385)$ resonance are sizable and, more importantly, whether they could modify the pattern of $V^{\rm CS30}_{K^-}$ and $V^{\rm CS30+phen.}_{K^-}$ established above. To this end we used the $\Sigma(1385)$-based p-wave potential of Weise and Härtle [18] consisting of resonance and background parts. While detailed account will be given elsewhere, we assert that fits to kaonic atom data within the present self-consistent procedure do not require substantial p-wave contributions, and that $V^{\rm CS30}_{K^-}$ and $V^{\rm CS30+phen.}_{K^-}$ are robust with respect to adding p waves.

[3] No similar bulge at the nuclear surface appears if $\mathrm{Im}\, V^{\rm CS30}_{K^-}$ is derived from CS30 'without SE' amplitudes, and $\mathrm{Im}\, V^{\rm CS30}_{K^-}(\rho_0)$ is then about twice that for the 'with SE' case shown in the figure.

Table 1
Binding energies B_K and widths Γ_K (in MeV) of 1s K^- nuclear quasibound states, calculated self consistently from Eq. (3) using in-medium 'with SE' CS30 amplitudes $F_{K^-N}(\sqrt{s},\rho)$ within a dynamical RMF scheme [14,25]. Possible $K^-NN \to YN$ ρ^2 contributions are excluded.

	^{12}C	^{16}O	^{40}Ca	^{90}Zr	^{208}Pb
B_K	54.8	54.9	68.2	77.3	82.2
Γ_K	11.7	11.4	9.8	9.4	8.6

4. K^-–nuclear quasibound states

The threshold K^-–nuclear potential $V^{\rm CS30}_{K^-}$ shown in Fig. 2 is sufficiently attractive to generate K^-–nuclear quasibound states. However, since the potential is energy dependent, it has to be calculated again self consistently for binding energies B_K in the expected range of tens of MeV. Calculations for ^{16}O and ^{208}Pb were reported by Weise and Härtle [18] using a subthreshold extrapolation

$$\sqrt{s} \approx E_{\rm th} - B_K - V_c \tag{10}$$

for solving self consistently the K^- KG equation within a local potential approximation of a chiral-model $\bar{K}N$ amplitude. The present self consistency scheme is based on Eq. (8) for $\sqrt{s}$ and Eq. (7) for k^2, as applied here to kaonic atoms, but without neglecting B_K for K^- nuclear states. We thus solved the KG equation (3), requiring self consistency explicitly for B_K (and implicitly for $\mathrm{Re}\, V_{K^-}$) using Eqs. (7) and (8). Realistic RMF density distributions $\rho(r)$ were employed, within a fully dynamical calculation that allows the nuclear density to get polarized by the K^- meson. In this dynamical scheme, following Refs. [14,25], a RMF self consistency cycle is applied in which the K^- meson solution serves further as a source in the RMF equations of motion which are solved to produce a modified nuclear density that goes again into the K^- meson KG equation. However, the present formulation differs fundamentally from previous RMF calculations: here V_{K^-} is generated microscopically from a two-body coupled channel chiral model and, furthermore, energy and density dependencies are introduced directly through the underlying K^-N scattering amplitude.

Binding energies and widths calculated dynamically for the 1s K^- nuclear quasibound state in several nuclei across the periodic table are listed in Table 1. The 'with SE' in-medium version of the CS30 chiral model was used. Similar results are obtained for the 'without SE' version, with slightly larger binding energies and widths. The values of B_K listed in the table are in close agreement with binding energies calculated within a dynamical RMF approach for nucleons and antikaons [25] when the K^- nuclear interaction is mediated exclusively by an ω vector field, with the same pure-F SU(3) coupling used in chiral models. The listed B_K values are smaller by 10–30 MeV than those calculated statically in Ref. [18]. We checked that applying the gauge-invariant substitution $\sqrt{s} \to \sqrt{s} - V_c$ in the r.h.s. of Eq. (8) makes little difference to the systematics of the binding energies and widths in Table 1, increasing B_K gradually between 1 MeV for ^{12}C to 5 MeV for ^{208}Pb. The real potential depths associated with the binding energies obtained here are of order 100 MeV (e.g. 110 MeV for the converged $\mathrm{Re}\, V_{K^-}$ in ^{40}Ca). They follow naturally from the strong energy dependence of $f_{K^-N}(\sqrt{s},\rho)$ at and below threshold which is incorporated within a genuinely self consistent and dynamical calculation of kaonic nuclei. The values of $f_{K^-N}(E_{\rm th},\rho)$, which for in-medium 'with SE' imply $\mathrm{Re}\, V_{K^-}(\rho_0) \approx -50$ MeV, are of no relevance to the actual binding energies of K^- nuclear quasibound states.

The calculated widths Γ_K listed in Table 1 represent only $K^-N \to \pi Y$ absorption processes that are accounted for by the coupled channels chiral model without allowing for multinucleon

Table 2
Binding energies B_K and widths Γ_K (in MeV) of the 1s K^- nuclear quasibound state in ^{16}O, calculated self consistently from Eq. (3) using in-medium CS30 amplitudes $F_{K^-N}(\sqrt{s},\rho)$ within a static RMF scheme for various prescriptions of treating $\sqrt{s}$. Unless stated to the contrary, the CS30 version is 'without SE'. Possible $K^-NN \to YN$ ρ^2 contributions are excluded.

	Eq. (10)	Eq. (8) − V_c	Eq. (8)	Eq. (8) + SE	+p waves
B_K	58.2	53.0	51.9	51.2	54.2
Γ_K	49.8	21.6	19.0	11.8	12.1

absorption modes. They are relatively small, of order 10 MeV, reflecting the proximity of the $\pi\Sigma$ thresholds which suppresses the major decay modes available for a K^- meson on a single nucleon. The sensitivity of the width calculation to the precise form of in-medium subthreshold extrapolation of $\sqrt{s}$ is demonstrated by five separate static calculations of the K^- 1s quasibound state in ^{16}O listed in Table 2. The first three calculations use the CS30 'without SE' version of the in-medium chiral model. The first one uses Eq. (10) for self consistency in the solution of the KG equation, mocking up as much as possible within our model the calculation by Weise and Härtle [18]. The next two calculations use Eq. (8) which shifts $\sqrt{s}$ further down with respect to where Eq. (10) shifts it, reducing Γ_K from about 50 MeV to about 20 MeV. The effect of subtracting V_c in the r.h.s. of Eq. (8), which yields the (B_K, Γ_K) values of the column marked 'Eq. (8) − V^c', is seen to be minor by comparing with the third (B_K, Γ_K) column. The last two calculations also use Eq. (8) for self consistency, but the CS30 in-medium version 'without SE' is replaced by 'with SE' which brings the calculated value of Γ_K further down to near its value in the dynamical calculation reported in Table 1. The last column includes also a $\Sigma(1385)$ p-wave contribution given in Ref. [18]. Its effect is found to be rather small since $\sqrt{s}$ is well below the peak of the $\Sigma(1385)$ resonance. A more detailed account of K^- quasibound state calculations incorporating p waves will be given elsewhere.

In addition to the $K^-N \to \pi Y$ single-nucleon induced widths of K^- quasibound states which are calculable from given in-medium chiral models and which were shown above to be quite model dependent, there are also sizable two-nucleon absorption processes $K^-NN \to YN$ with considerably lower thresholds that contribute additional widths of order 40 MeV [14,18,25]. These absorption processes could be simulated by adding energy dependent imaginary ρ^2 terms suggested by the (CS30 + phen.) potential for kaonic atoms together with the associated dispersive real ρ^2 terms. This requires further consideration.

5. Conclusion

In conclusion, we have shown within in-medium extensions of the chirally motivated coupled-channel separable-interaction CS30 model [17] how to incorporate the strong energy and density dependence of the K^-N scattering amplitude $F_{K^-N}(\sqrt{s},\rho)$, at and below threshold, into a self consistent evaluation of the SE operator $\Pi_K(\omega_K,\rho)$ for kaonic atoms. The procedure adopted here is sufficiently general to be applied within in-medium extensions of other chirally motivated interaction models. Our calculations demonstrate that kaonic atom data probe the subthreshold regime of the in-medium K^-N scattering amplitude. The two in-medium extensions of CS30 considered in the present work produce parameter-free K^- nuclear potentials for kaonic atoms which are similar to each other, with depths $-\mathrm{Re}\,V_{K^-}^{\mathrm{CS30}}(\rho_0) = (85\pm5)$ MeV and $-\mathrm{Im}\,V_{K^-}^{\mathrm{CS30}}(\rho_0) = (20\pm10)$ MeV evaluated at the center of a typical medium-weight nucleus such as Ni. Preliminary calculations using the Tomozawa–Weinberg lowest order chiral interaction term, including the new SIDDHARTA 1s level shift and width in kaonic hydrogen [26] produce similar results. The sharp decrease of $\mathrm{Im}\,f_{K^-N}$ towards the $\pi\Sigma$ threshold is reflected in rapid decrease of $\mathrm{Im}\,\mathcal{F}_{K^-N}^{\mathrm{eff}}$ with increased density. Therefore absorption processes beyond a single nucleon mechanism must be added together with a possible dispersive real term. Indeed to achieve truly low χ^2 values for K^- atoms, phenomenological potential terms had to be added, leading to increased V_{K^-} depths, i.e., $-\mathrm{Re}\,V_{K^-}^{\mathrm{CS30+phen.}}(\rho_0) = (180\pm5)$ MeV and $-\mathrm{Im}\,V_{K^-}^{\mathrm{CS30+phen.}}(\rho_0) = (70\pm20)$ MeV. These dominantly ρ^2 terms could represent K^-NN processes outside of the present single-nucleon chiral model.

K^- nuclear quasibound states generated by in-medium extensions of CS30 were also calculated within a self consistent scheme. Potential depths $-\mathrm{Re}\,V_{K^-}(\rho_0)$ of order 100 MeV were obtained for both extensions used, exceeding somewhat the depths derived for kaonic atoms. This indicates a moderate state, or energy dependence of $\Pi_K(\omega_K,\rho_0)$. The similarity of the results for the two in-medium extensions used here is in striking contrast to the large difference in their $\mathrm{Re}\,f_{K^-N}$ values at threshold, as can be judged from Fig. 1. Implementing additional phenomenological terms within K^- nuclear quasibound calculations is likely to result in B_K values higher than 100 MeV. This topic deserves further consideration.

Our calculations provide for the first time a microscopic link between shallow K^- nuclear potentials [5,23] obtained from threshold K^-N interactions and phenomenological deep ones deduced from kaonic atom data [13,14]. In future work, p-wave $\bar{K}N$ subthreshold amplitudes associated with the $\Sigma(1385)$ resonance will be explored in detail, to confirm the secondary role played by these amplitudes in our preliminary extended studies of kaonic atoms[4] and in studies of quasibound K^- nuclear states [18,25].

Acknowledgements

Stimulating discussions with Wolfram Weise are gratefully acknowledged. This work was supported by the GACR Grant No. 202/09/1441, as well as by the EU initiative FP7, HadronPhysics2, under Project No. 227431.

References

[1] See: A. Gal, R.S. Hayano (Eds.), Special Issue on Recent Advances in Strangeness Nuclear Physics, Nucl. Phys. A 804 (2008), pp. 171–348.
[2] W. Weise, Nucl. Phys. A 835 (2010) 51, and references therein;
T. Hyodo, D. Jido, Prog. Part. Nucl. Phys., submitted for publication, arXiv:1104.4474 [nucl-th].
[3] J. Schaffner-Bielich, S. Schramm, H. Stöcker, in: M. Anselmino, et al. (Eds.), Proc. Int. School of Physics "Enrico Fermi", Course CLXVII, IOS Press, Amsterdam, 2008, pp. 119–144;
F. Özel, G. Baym, T. Güver, Phys. Rev. D 82 (2010) 101301(R).
[4] T. Waas, N. Kaiser, W. Weise, Phys. Lett. B 365 (1996) 12;
T. Waas, N. Kaiser, W. Weise, Phys. Lett. B 379 (1996) 34.
[5] A. Ramos, E. Oset, Nucl. Phys. A 671 (2000) 481.
[6] Y. Akaishi, T. Yamazaki, Phys. Rev. C 65 (2002) 044005;
T. Yamazaki, Y. Akaishi, Phys. Lett. B 535 (2002) 70.
[7] M. Agnello, et al., FINUDA Collaboration, Phys. Rev. Lett. 94 (2005) 212303.
[8] T. Yamazaki, et al., DISTO experiment, Phys. Rev. Lett. 104 (2010) 132502.
[9] A. Cieplý, E. Friedman, A. Gal, V. Krejčiřík, Phys. Lett. B 698 (2011) 226.
[10] M. Agnello, et al., FINUDA Collaboration, Phys. Lett. B 698 (2011) 219.
[11] T. Sekihara, D. Jido, Y. Kanada-En'yo, Phys. Rev. C 79 (2009) 062201.
[12] E. Friedman, A. Gal, Phys. Rep. 452 (2007) 89.
[13] E. Friedman, A. Gal, C.J. Batty, Phys. Lett. B 308 (1993) 6;
E. Friedman, A. Gal, C.J. Batty, Nucl. Phys. A 579 (1994) 518.
[14] J. Mareš, E. Friedman, A. Gal, Nucl. Phys. A 770 (2006) 84.
[15] S. Wycech, Nucl. Phys. B 28 (1971) 541.

[4] See also Ref. [27] for a related calculation using threshold amplitudes.

[16] W.A. Bardeen, E.W. Torigoe, Phys. Lett. B 38 (1972) 135.
[17] A. Cieplý, J. Smejkal, Eur. Phys. J. A 43 (2010) 191.
[18] W. Weise, R. Härtle, Nucl. Phys. A 804 (2008) 173.
[19] B. Borasoy, U.-G. Meißner, R. Nißler, Phys. Rev. C 74 (2006) 055201.
[20] T. Hyodo, W. Weise, Phys. Rev. C 77 (2008) 035204.
[21] A. Cieplý, E. Friedman, A. Gal, J. Mareš, Nucl. Phys. A 696 (2001) 173.
[22] M. Lutz, Phys. Lett. B 426 (1998) 12.
[23] A. Baca, C. García-Recio, J. Nieves, Nucl. Phys. A 673 (2000) 335.
[24] M. Ericson, T.E.O. Ericson, Ann. Phys. 36 (1966) 323. For a recent review see Ref. [12].
[25] D. Gazda, E. Friedman, A. Gal, J. Mareš, Phys. Rev. C 76 (2007) 055204;
D. Gazda, E. Friedman, A. Gal, J. Mareš, Phys. Rev. C 77 (2008) 045206;
D. Gazda, E. Friedman, A. Gal, J. Mareš, Phys. Rev. C 80 (2009) 035205.
[26] M. Bazzi, et al., SIDDHARTA Collaboration, Phys. Lett. B, submitted for publication, arXiv:1105.3090 [nucl-ex].
[27] C. García-Recio, J. Nieves, E. Oset, A. Ramos, Nucl. Phys. A 703 (2002) 271.